Volume 213, 15 September 2013 ISSN 0920-5861

ELSEVIER

CATALYSIS TODAY

Selected contributions of the XXIII Iberoamerican Congress on Catalysis

Guest Editors
Juana Isabel Di Cosimo and Carlos R. Apesteguía

Journal Homepage:
www.elsevier.com/locate/cattod

Available online at www.sciencedirect.com
SciVerse ScienceDirect

Catalysis Today 213 (2013) 171–182

Contents lists available at SciVerse ScienceDirect

Catalysis Today

journal homepage: www.elsevier.com/locate/cattod

Cooper foils used as support for catalytic monoliths. Superficial nano/microstructures obtained for two treatments

Maria R. Morales*, Luis E. Cadus

Instituto de Investigaciones en Tecnología Química (INTEQUI), Universidad Nacional de San Luis – CONICET, Chacabuco y Pedernera, 5700 San Luis, Argentina

A R T I C L E   I N F O

Article history:
Received 8 November 2012
Received in revised form 15 March 2013
Accepted 19 March 2013
Available online 20 May 2013

Keywords:
Metallic monolith
Copper
Chemical treatment
Thermal treatment
Combustion
Toluene

A B S T R A C T

Copper metallic monoliths were thermally and chemical treated. Copper oxides with different nano/microstructures were obtained applying different variables in both treatments. They showed to be stable and suitable to act as support of the Mn9Cu1 catalyst bulk or as an active catalytic phase. Two monoliths representing each treatment were evaluated in the combustion of toluene. Both showed a good performance.

1. Introduction

Catalytic oxidation is the most attractive way to eliminate volatile organic compounds (VOCs) at low concentration in industrial gaseous effluent. The catalysts based on transition metal oxides have shown to be an interesting alternative to replace those based on noble metals since they are less expensive and less sensitive to poisoning [1,2]. For practical applications, the catalyst should be supported on a structured support to treat large gas flows with low pressure drop. The most widely used structured supports are monoliths with longitudinal parallel channels made of ceramic or metallic materials. The most popular supports with monolithic structure are the ceramic ones, due to their extended use in the automobile sector [3]. Although metallic monoliths are more expensive than ceramic ones, they present a less thick wall (25–50 μm) and a higher thermal conductivity. However, the low adherence of the washcoating acting as support of the active phase constitutes their main disadvantage. This problem can be solved by several chemical modifications in the preparation of the washcoating, and by the use of metals or alloys chemically and/or thermally treated. They form an oxide layer adherent and stable that acts as anchor of the coating [4].

Many different metals and alloys have been proposed for the manufacturing of metallic monoliths such as Ni–Cr alloys, ferritics steel alloys containing Al, stainless steel (AISI 304, AISI 316) and aluminium, among others.

It has been reported that in aluminium steel (FeCrAlloy) [5,6] and stainless steel (AISI 304) [7], the adherent oxide layer is achieved by a heat treatment. In aluminium foil, a layer of alumina is obtained through an anodization process. Sulphuric acid is used as electrolyte [5,8,9]. In alloys of Ni–Cr chemical treatments with a mixture of HCl–H_2SO_4 have been used. Such treatment provides a surface roughness to the sheet [10]. This surface roughness favours the later deposition of the active phase.

Copper is widely used in many industrial applications. Due to the behaviour of p-type semiconductor with a narrow band gap (1.2 eV), CuO has potential applications in many fields, such as superconductors [11,12], gas sensors [13,14], heterogeneous catalysts [15], magnetic storage media [16] and lithium-ion electrode materials [17]. Particularly, some of CuO nanostructures have received considerable attention due to their new physical and chemical properties that are not available from bulk CuO [17–22].

Mn–Cu catalysts, bulk and supported on metal monoliths, have been widely studied in the working group. They showed excellent catalytic activity in combustion of many VOCs [23,24]. The possibility that a copper substrate is used as a construction material of monoliths facilitates the preparation of these mixed catalysts. A simple impregnation with a precursor of manganese would obtain these mixed catalysts. However, it would be also interesting to seek

---

* Corresponding author. Tel.: +54 (0)266 424689x116; fax: +54 (0)266 426711.
E-mail address: mrmorale@unsl.edu.ar (M.R. Morales).

0920-5861/$ – see front matter © 2013 Elsevier B.V. All rights reserved.
http://dx.doi.org/10.1016/j.cattod.2013.03.036

texture characteristics that favour the deposition of the catalyst by washcoating. Mainly, it would require a stable surface roughness which allows the anchoring of catalyst particles.

Copper is not chemically stable when exposed to air and water. Different methods have been used to generate copper oxide nanostructures, from foils of copper. Such as thermal oxidation [18,25], wet chemical methods [17,20,26,27], reaction between thermally evaporated Cu and O_2 plasma [28], among others.

Zhang et al. [29] carried out surface oxidation on copper substrates in alkaline aqueous solutions (NaOH or $NaHCO_3$) with $(NH_4)_2S_2O_8$, at room temperature and pressure. They applied modified variables such as: pH, NaOH concentration and reaction time. They observed the formation of $Cu(OH)_2$ fibres and scrolls, and CuO sheets and whiskers, perhaps due to the dehydration of $Cu(OH)_2$. In a subsequent paper [22], they obtained thicker and aligned $Cu(OH)_2$ nanostructures lowering the temperature at 0 °C. But as a result of using lower growth temperature, the reaction time was increased (10 h).

Zhang et al. [29] and Shang et al. [30] obtained nanostructures corresponding only to CuO phase. Zhang et al. [29] worked at room temperature and pressure, using $[NaOH]–[(NH_4)_2S_2O_8]$ as alkaline-oxidant medium. Moreover, Shang et al. [30] used $[KOH]–[H_2O_2]$ as alkaline-oxidant medium, and the treated foils were dried at 60 °C.

Shang et al. [30] could predict the possible growth mechanism for the formation of straw-like CuO nanostructures. The formation of $Cu(OH)_2$ nuclei in this process was not fast and the precipitation started when H_2O_2 had a proper environment (temperature and time) to generate Cu^{2+}. It reacted with KOH for the formation of $Cu(OH)_2$ nuclei. The possible chemical reactions are written down below:

$$H_2O_2 \rightarrow H_2O + O_2 \quad (1)$$

$$Cu + OH^- \rightarrow Cu(OH)_2 + H_2O \quad (2)$$

$Cu(OH)_2$ initially formed gets dehydrated in situ rapidly and then converted completely into CuO in the heating process. The equation of the chemical reactions is given by

$$Cu(OH)_2 \rightarrow CuO + H_2O \quad (3)$$

Yu et al. [26] synthesized flower-like cupric oxide nanostructures (CuO nanoflowers) directly on Cu plates in KOH solution at room temperature. In their experiment, no strong oxidant was intentionally used. Nonetheless, O_2 in the solution, even in small proportion, could play the role of oxidant. They suggested the formation of $[Cu(OH)_4]^{2-}$ anion as the first stage of reaction mechanism. It can be considered a precursor for the formation of CuO. Solid CuO as a result of condensation of these complexes was obtained. Under these conditions, the absence of an oxidizing agent modified the treatment time, which was approximately 2 weeks. Although this treatment would imply a lower cost and a smaller amount of liquid waste, treatment times are too long to generate nanostructures suitable for achieving the aims proposed in this paper.

The thermal treatment is probably the most used technique to produce copper nanostructures [18,31,32]. Oxidative atmospheres, oxygen partial pressures, temperatures and treatment time generate different copper nanostructures.

It has been reported that the morphology of the oxides formed depends on the oxygen partial pressure applied. Also, the water steam present in the oxidizing atmosphere has an effect on the growth of nanostructures [31–34]. Xu et al. [33] worked with air (dry–wet), nitrogen with traces of oxygen (dry–wet), and oxygen (dry–wet). They observed that with oxygen atmosphere, nanostructures of a greater density (nanotubes) are formed. The presence of water steam in the oxidizing atmosphere significantly affects the formation of nanotubes. While the nanotube density was higher in wet air, when the atmosphere was wet oxygen, a decrease in the density was observed. During the use of air (dry–wet), Cu_2O was obtained as the main phase, accompanied by a small amount of CuO. When nitrogen with traces of oxygen was used, the formation of nanotubes in both dry and wet atmospheres was not observed. Cu_2O was the only phase identified.

When the temperature of treatment was the variable used, the formation of nanostructures was observed only between 400 and 700 °C. At temperatures below 400 °C, a surface covered with particles or grains of Cu_2O was reported. A dense layer of high crystallinity micron particles (CuO) was observed on the surface, at temperatures above 700 °C. At 400 °C and 500 °C nanotubes of mixed phases (Cu_2O–CuO) were detected, predominating the CuO phase. At 600 °C a high density of nanotubes was reported, being more uniform and stronger than those obtained at lower temperatures [18,31,35,36].

The increase in temperature causes a decrease of the density of nanotubes, but these are stronger because their diameter increases [31]. Moreover, the growth time variation influences the density and length of the nanotubes, but not their diameters. The increase of this variable causes the reduction of the growth rate [36].

Table 1
Chemical treatment conditions and nomenclature of supports monoliths.

Molar relationships $[NaOH]/[H_2O_2]$	[NaOH] (M)	Reaction time (h)	Nomenclature
10	1	24	10-1-24
10	1	40	10-1-40
10	2	24	10-2-24
10	2	40	10-2-40
10	6	24	10-6-24
40	2	40	40-2-40
40	6	40	40-6-40

Table 2
Thermal treatment conditions and nomenclature of supports monoliths.

Atmosphere	Temperature (°C)	Time (min)	Nomenclature
Stagnant	500	5	S55
		15	S515
		30	S530
	600	5	S65
		15	S615
		30	S630
Dry air	500	5	DA55
		15	DA515
		30	DA530
	600	5	DA65
		15	DA615
		30	DA630
Wet air	500	5	WA55
		15	WA515
		30	WA530
	600	5	WA65
		15	WA615
		30	WA630
Dry oxygen	500	5	DO55
		15	DO515
		30	DO530
	600	5	DO65
		15	DO615
		30	DO630
Wet oxygen	500	5	WO55
		15	WO515
		30	WO530
	600	5	WO65
		15	WO615
		30	WO630

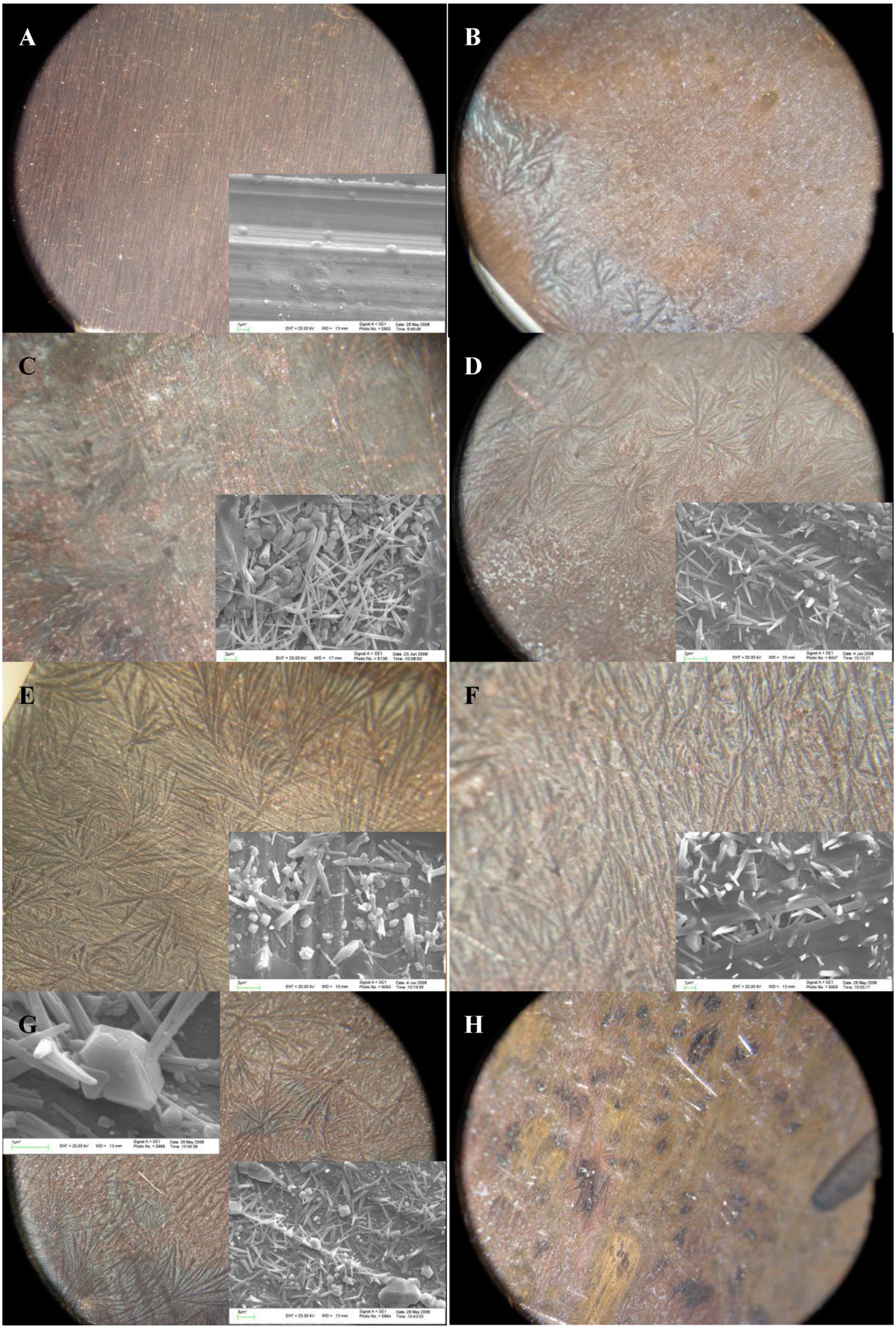

Fig. 1. Photos magnifier and SEM images of the support monoliths: (A) Cu°; (B) 10-1-24; (C) 10-1-40; (D) 10-2-24; (E) 10-2-40; (F) 10-6-24; (G) 40-2-40 and (H) 40-6-40.

The surface morphology achieved from these treatments would solve the problem of the low adhesion in metal monoliths, due to the non-porous nature of metal foils. For catalytic application of the copper foils proposed in this paper, the treatments should be modified, and the number of variables applied should be reduced. By this treatment, optimal nanostructures for our purposes would be obtained, achieving a compromise between the amount and type of nanostructures generated and stability.

The main objective of this paper is to study both the possibility to generate stable nanostructures from the surface of the Cu foil, applying thermal and chemical treatments; and the feasibility to use the nanostructures formed as anchorage of catalyst particles or as the active phase for combustion reactions.

2. Experimental

2.1. Preparation of monolithic catalysts

2.1.1. Manufacture of the bare monoliths

Monoliths were made of copper with a purity of 99.9% (Goodfellow). The copper monoliths were prepared from thin foils (0.05 mm thick) by rolling around spindle alternate flat and crimped foils. The dimensions of the monoliths were: 3 cm long and 1.6 cm in diameter; 330 cpi.

2.1.2. Cleaning of the monoliths

Remaining oil and other impurities on the surface of the copper foils from the maching step were eliminated by successive washes in ultrasound. First they were washed in HCl (1 M) for 1 min, then in distilled water for 10 min and finally in ethanol for 10 min, the last two steps were repeated once more. Finally the foils were dried in air flow for 10 min.

2.2. Treatment of the metal support

2.2.1. Chemical treatment

Aqueous solutions of sodium hydroxide 10 M and peroxide 1 M were prepared. Adequate amounts of each of the solutions were mixed obtaining the molar relationships: $[NaOH]/[H_2O_2] = 10$ and 40 for a concentration of sodium hydroxide: $[NaOH] = 1, 2,$ and 6 M respectively. Each mixture was carried to a total volume of 15 ml with distilled water.

Monoliths were immersed in the solution. This solution was recirculated during 24 and 40 h with a peristaltic pump. Then monoliths were dried in air for 10 min. The nomenclature used for these support monoliths was: $[NaOH]/[H_2O_2]$–[NaOH]–time. Table 1 shows the treatment conditions and the nomenclature of each monolith.

2.2.2. Thermal treatment

Monoliths were treated in five atmospheres: stagnant atmosphere (S), dry air (DA), wet air (WA), dry oxygen (DO) and wet oxygen (WO); two temperatures, 500 °C (5) and 600 °C (6) and three times; 5, 15 and 30 min.

Monoliths were placed in a quartz reactor in a horizontal furnace. A heating rate of 50 °C min^{-1} and a constant flow rate were used. A humidity of 60% in humid atmospheres was employed. Monoliths were named as: atmosphere–temperature–time. Table 2 presents the conditions of treatment and nomenclature.

2.2.3. Washcoating with the ready-made Mn9Cu1 catalyst

Mn9Cu1 catalyst was obtained as a powder by the coprecipitation method from $Mn(NO_3)_2·4H_2O$ and $Cu(NO_3)_2·4H_2O$ with a molar ratio Mn:Cu = 9:1. The details of the synthesis procedure and characterization results were presented in a previous paper [23]. The optimal conditions for preparing the suspension were determined in another work [37]. Taking into account those results, the powder Mn9Cu1 catalyst was milled for 9 h for a characteristic particle size d_{90} (90% of the particles of the batch are smaller than that) of 4.5 μm. Then, an aqueous suspension with 35 wt% solid content adding colloidal alumina (Nyacol® Al20) as stabilizer was prepared. The pH = 4 was adjusted using diluted HNO_3. The slurries were subjected to orbital agitation for 17 h before being used for washcoating. A copper monolith was dipped into the slurry for 10 s, withdrawn at constant speed of 3 cm min^{-1} and then, the suspension excess was eliminated by blowing air for 1 min. To remove suspension in excess, Barbero et al. [37] used centrifugation, in this work this step was replaced by blowing air, considering the future scale up of the monoliths. Finally, it was dried at 120 °C for 1 h and calcined at 250 °C for 2 h and at 500 °C for 3 h. This monoliths were denoted as 10-2-24 + Mn9Cu1 and 530 + Mn9Cu1.

2.3. Characterization techniques

2.3.1. X-ray diffraction (XRD)

XRD patterns were obtained by using a Rigaku diffractometer with a radiation source Ni-filtered Cu Kα (λ = 0.1541 nm) over a 20–80° 2θ-range and a position-sensitive detector with 0.05° step size at a scan rate of 1° min^{-1}.The crystalline phases were identified by reference to powder diffraction data (PDF-ICDD).

2.3.2. Scanning electron microscopy (SEM)

The morphology of samples was examined with a scanning electron microscope LEO 1450VP. This instrument is equipped with an

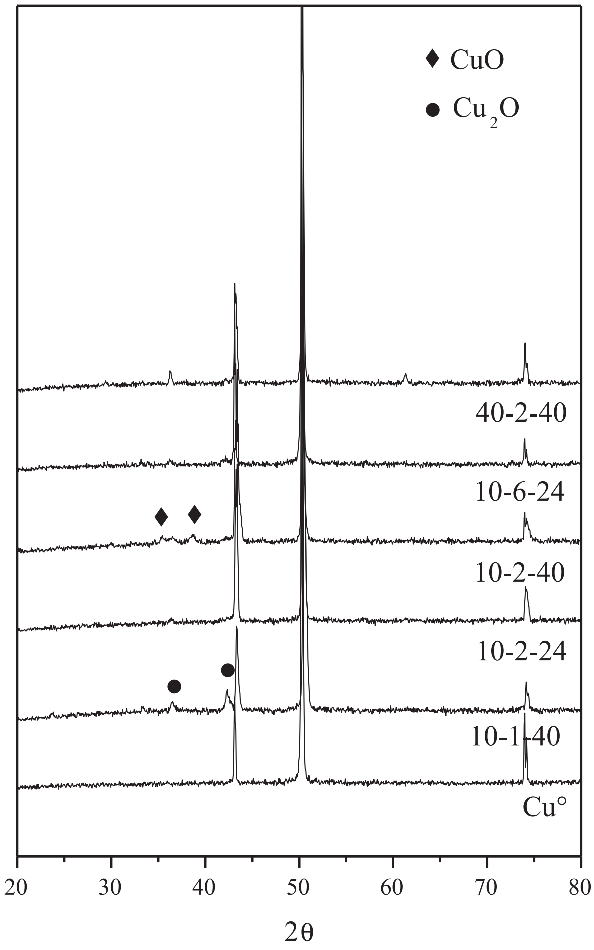

Fig. 2. XRD patterns of the support monoliths obtained by chemical treatment.

energy-dispersive analyzer of X-rays EDAX Genesis 2000 with Si (Li) detector.

2.3.3. *BET surface area*

The surface area of monoliths was measured by the BET method from the nitrogen adsorption isotherms obtained at 77 K on samples outgassed at 393 K using a Micromeritics Gemini V apparatus. A home-made cell was used for the measurement of complete monoliths.

2.3.4. *Adherence test*

The adherence of the deposited phase was evaluated in terms of the weight loss after exposure of the monoliths to ultrasonic vibration following the procedure described in the literature [38]. The monoliths were immersed in petroleum ether, inside a sealed beaker, and then treated in an ultrasound bath for 30 min. After that, the monoliths were dried at 80 °C for 2 h. The weight loss was gravimetrically determined measuring the weight of the samples both before and after the ultrasonic treatment.

2.3.5. *Catalytic test*

The monoliths were evaluated in toluene combustion. The feed concentration was 4000 mgC m^{-3}. The total flow was 300 ml min^{-1} resulting in a space velocity of 3000 h^{-1}. The reactives and reaction products were analysed by on-line gaseous chromatography using a Buck Scientific Mod 910 chromatograph equipped with a FID detector, a methanizer and a Carbowax 20M on Chromosorb W column.

The conversion, X%, was defined as the percentage of VOC feed that reacted. Since the catalyst loading can differ in monolithic catalysts, the catalytic performances are also expressed in terms of intrinsic catalytic activity (moles of converted VOCs $g^{-1}\,h^{-1}$) according to the following equation:

$$\frac{\text{mol}}{\text{g h}} = \frac{X_{\text{VOCs}} \times F}{m_{\text{cat.}} \times 100}$$

where X_{VOCs} represents the conversion rate of VOCs at a given temperature (%); F, the VOCs flow ($\text{mol}_{\text{VOCs}}\,h^{-1}$); and $m_{\text{cat.}}$, the catalyst mass deposited on the monolith (g).

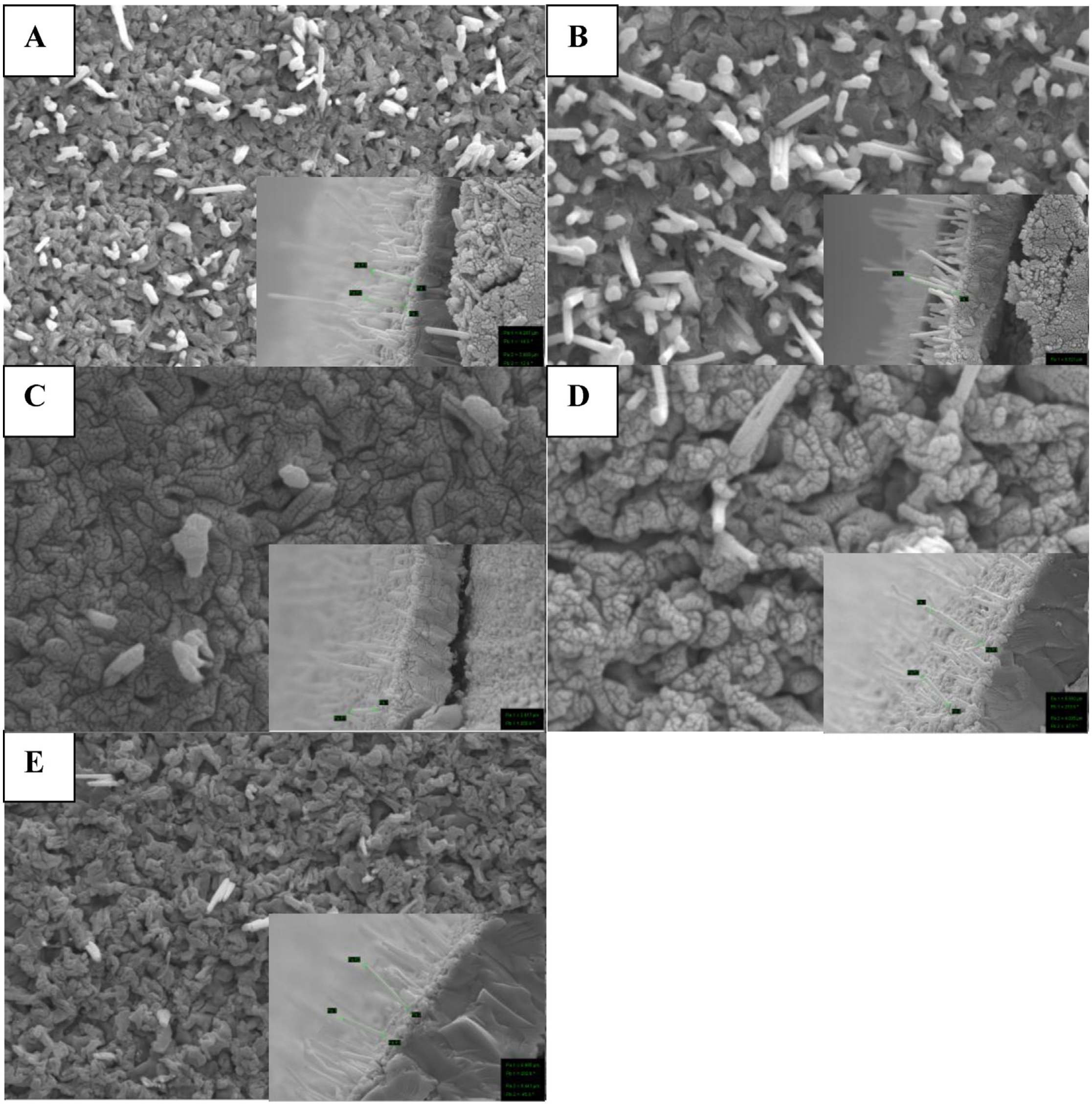

Fig. 3. SEM images of the support monoliths obtained by thermal treatment: (A) DA55; (B) DA515; (C) DA530; (D) DA615 and (E) DA630. Atmosphere: dry air. Temperature: 500 and 600 °C and time: 5, 15 and 30 min.

3. Results and discussion

Zhang et al. [29] reported a chemical treatment on copper foils thicker than those of this work, using ammonium persulfate as oxidant. The treatment variables of their work were: pH, concentrations of NaOH and reaction times of the solution with the foil. They observed that, with [NaOH] = 1–5.5 M and a molar ratio of [NaOH]/[$(NH_4)_2S_2O_8$] maintained between 10 and 40, a blue film was easily formed on the foil surface. The Scanning Electronic Micrograph (SEM) showed that this film was constituted by $Cu(OH)_2$ fibres. With reaction times higher than 10 h, they observed the transformation of the film colour from blue to black due to the rapid dehydration of $Cu(OH)_2$, generating CuO.

Taking into account the results reported by Zhang et al. [29], a chemical treatment on Cu monoliths at room temperature and pressure was carried out. Hydrogen peroxide was used as oxidant agent since its oxidant power is similar to that of $(NH_4)_2S_2O_8$ in order to avoid a possible poisoning of the surface by sulphur residues derived from ammonium persulphate. The assays were carried out at: pH > 13, [Na(OH)]/[H_2O_2] = 10 and 40, [Na(OH)] = 1, 2 and 6 M, and reaction times = 24 and 40 h. According to the current literature, these conditions would guarantee the formation of stable surface nano/microstructures.

Fig. 1 shows optical microscope photographs with SEM details of copper monoliths after the chemical treatment. The homogeneity of the attack and the generation of copper nano/microstructures on the foil surface can be observed. The conditions used for 10-1-40 and 40-6-40 support monoliths did not generate a homogeneous attack on the surface. Zones with a dark colouration, where the attack was more vigorous were observed. Due to the possibility that these zones would facilitate a detachment of the layer of copper nano/microstructures, the treatment conditions applied to 10-1-40 and 40-6-40 support monoliths were not selected. For the rest of the chemical treatment conditions, the formation of needle-like crystals and others of different morphology, mainly of an irregular octahedral structure was detected. Lv et al. [39] also observed this type of structure but they performed a chemical treatment assisted by cationic/anionic surfactants in autoclave.

The constituent phases of these generated nano/microstructures were determined by X-ray diffraction

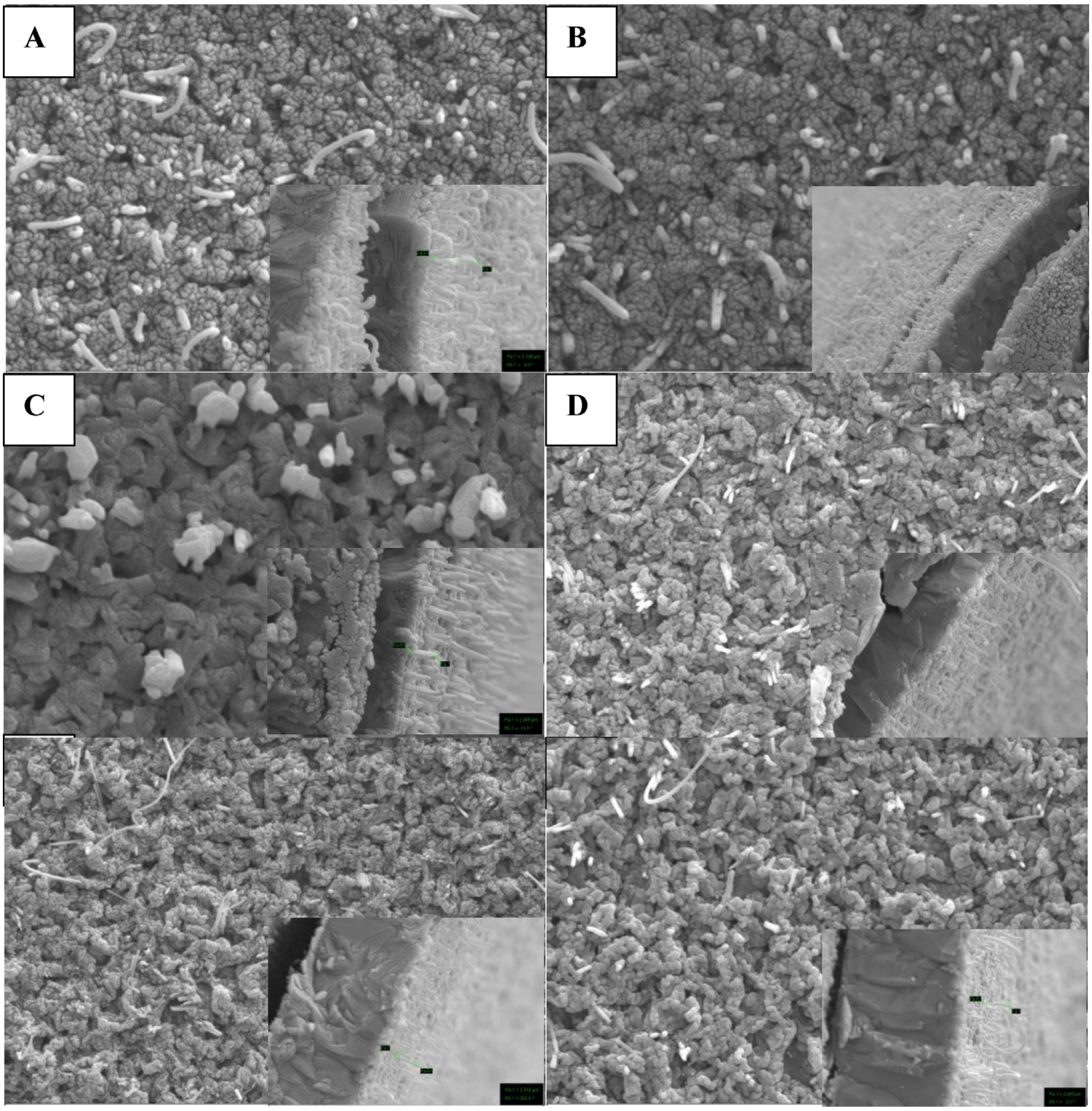

Fig. 4. SEM images of the support monoliths obtained by thermal treatment: (A) DO55; (B) DO515; (C) DO530; (D) DO65; (E) DO615 and (F) DO630. Atmosphere: dry oxygen. Temperature: 500 and 600 °C and time: 5, 15 and 30 min.

(Fig. 2). The lines of diffraction corresponding to Cu_2O (PDF 5-667) were identified in all the support monoliths and lines of CuO oxide (PDF 5-661) were observed only in 10-2-40 support monolith. This is a surprising result not consistent with the observations made by Zhang et al. [29], Shang et al. [30] and Jana et al. [40]. They obtained CuO as the main phase under reaction conditions similar to those applied in this work. The generation of Cu_2O as the major phase in the monoliths under study could be associated to: (a) the use of hydrogen peroxide as oxidant agent and (b) the post-attack treatment, since monoliths are dried at room temperature. After the treatment, Shang et al. [30] and Jana et al. [40] dried the foils for 3 or 4 h at 60 °C. According to the growth mechanism of Cu nanostructures proposed by Shang et al. [30], the dehydration showed in Eq. (3) (Section 1) may be slower, not reaching the formation of CuO with the drying conditions used in this work. In fact, the X-ray diffraction results show that, for low reaction times (24 h) and $[NaOH]/[H_2O_2] = 10$, only an increase in the intensity of diffraction lines of the Cu_2O phase is observed; while for the same molar ratio and $[NaOH] = 2\,M$, the increase in the reaction time facilitates the formation of CuO phase which is also favoured by an increase in H_2O_2 and NaOH concentrations, i.e. more vigorous conditions of reaction.

The new phase morphology generated on the surface of the copper monoliths is very important to evaluate their use as anchorages of catalysts. The SEM micrographs in Fig. 1 show that, for longer reaction times (40 h), needle-like nano/microstructures of greater diameter and a higher amount of irregular octahedral crystals are obtained. In line with this, Zhang et al. [29] reported that with the increase of treatment time from 0.5 h to 9 h, the $Cu(OH)_2$ fibres obtained incremented their diameter and density.

With high concentrations of the oxidant agent and alkalis, needle-like nano/microstructures of a greater length and diameter are observed, and the crystals with irregular octahedral structure are better defined but in a smaller proportion. Shang et al. [30] and Yu et al. [26] observed the same effect on CuO straw-like nanostructures with the increase of concentration (KOH). These authors considered that alkali played a crucial role in the formation of the nanostructures, favouring the process of nucleation. However, they observed that the concentration of the oxidant agent (H_2O_2) did not have any effect on the morphology of nanostructures since the

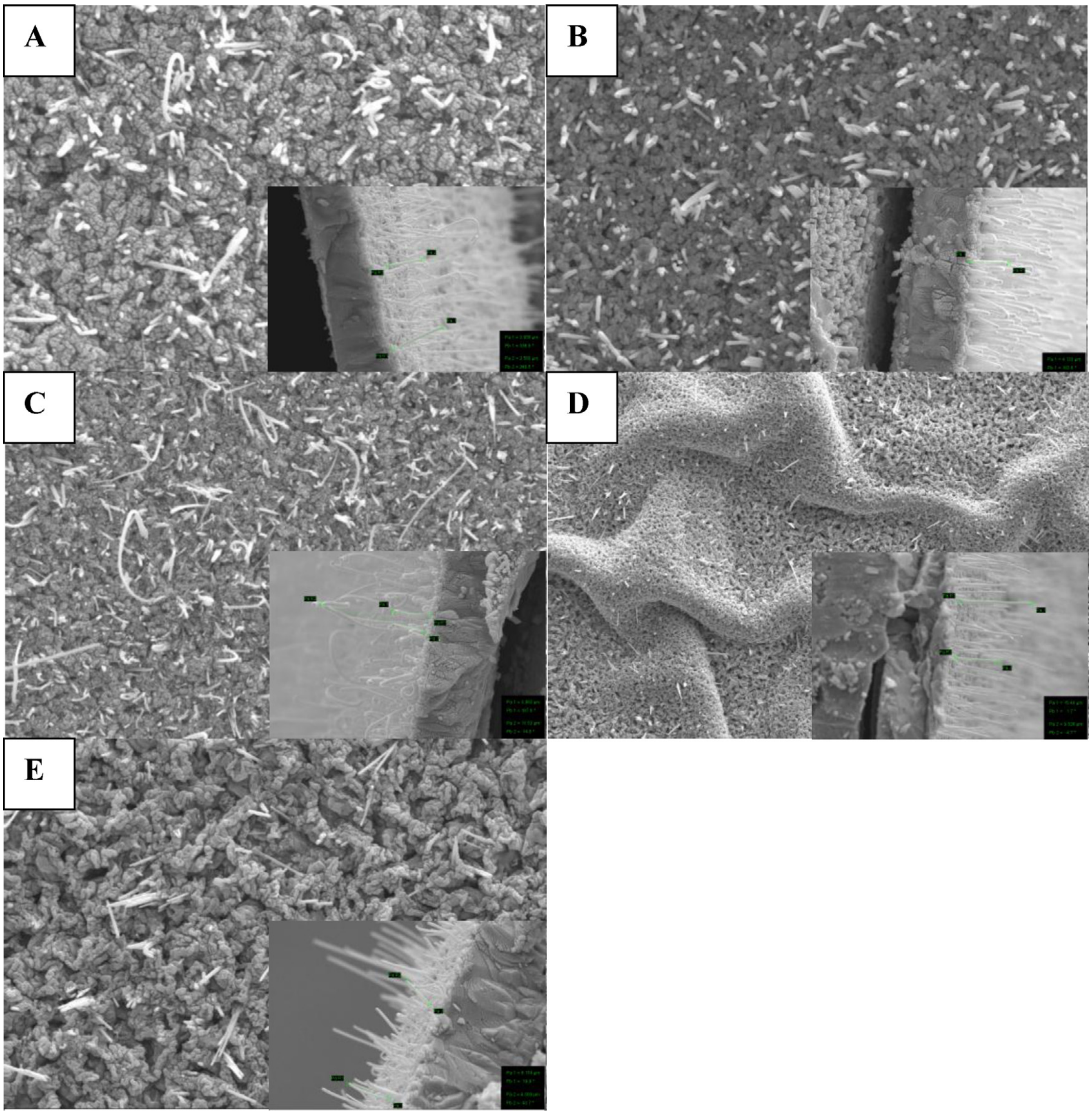

Fig. 5. SEM images of the support monoliths obtained by thermal treatment: (A) WA55; (B) WA515; (C) WA530; (D) WA615 and (E) WA630. Atmosphere: wet air. Temperature: 500 and 600 °C and time: 5, 15 and 30 min.

diameters and lengths did not vary significantly, contrary to the observations in this work.

The spaces between the nano/microstructures generated in all the support monoliths ranged from 2 μm to 6 μm, approximately, making them suitable for the deposition of a catalyst by washcoating. However, the functionality existing between the diameter-length of the nano/microstructures and their fragility has to be taken into account. This is a direct measure of the stability of the surface morphology attained.

The thermal treatment of copper foils is simpler than the chemical treatment, and it also has the advantage of being a clean technique since it does not generate liquid waste, contributing to the so-called "green chemistry."

On the basis of the information reported in the literature [33,35,36], the variables applied to the thermal treatment in this work were the following: oxidative atmosphere (stagnant, air, oxygen – dry and wet), temperature (500–600 °C), and treatment time (5–15–30 min). These parameters strongly modify the structural characteristics (length and diameter) and the type of nano/microstructures that can be generated. As previously mentioned, the selection of these variables was aimed at obtaining stable nano/microstructures which would lead to a surface morphology appropriate for the catalytic objectives proposed.

With the thirty possible combinations of variables applied to the thermal treatment, the formation of copper microstructures was mainly observed. These microstructures were wire-like, with different lengths, diameters and growth densities, depending on the variables applied.

It has been shown that growth time may be used for controlling the distribution of lengths of CuO nanostructures while growth temperature, for controlling the distribution of diameters. Additionally, the partial pressures of H_2O and O_2 affect significantly the nanostructure density [33,34].

In Figs. 3 and 4, a decrease in microwire density with the increase of growth time and temperature is observed, especially for 30 min with dry atmosphere (air and oxygen). Chen et al. [35] and Huang et al. [36] observed an increment of nanostructure density and length with the increase of growth time for these atmospheres. The discrepancy with our results may be due to the fact that these authors used longer growth times (0.5–8 h). However, the effect of temperature is similar to theirs.

The effect of assisting the nucleation on the formation of nanostructures has been attributed to water steam. In fact, in wet atmospheres (Figs. 5 and 6) with the increase of growth time, the density and length of microwires are higher. Contrarily, with the rise of temperature, the density as well as length decreases.

Fig. 7 shows SEM micrographs for a stagnant atmosphere. With the increase of growth time, the generated microstructures disappear, and a granulated surface is obtained. Instead, with the rise of temperature, the microstructure density generated at short times is lower.

The copper oxide nanostructured films present serious problems of cracking or flaking due to the tension existing between the oxide layer and the substrate [35,41]. This phenomenon is favoured by the presence of water steam in the atmosphere. In Figs. 3, 5 and 6, the SEM micrographs do not show supports having detachments of the generated oxide layer

In general terms, with the increase of the oxygen content of the atmosphere, the density and length of nano/microstructures are higher. Elevated partial pressures of oxygen improve the possibility of nucleation; specifically they improve the rate of nano/microstructure growth and also, they have effect on the morphology of the generated oxides [33].

As for the support monoliths obtained by chemical treatment, the spaces generated between the microwires are suitable for the physical anchorage of active phase particles.

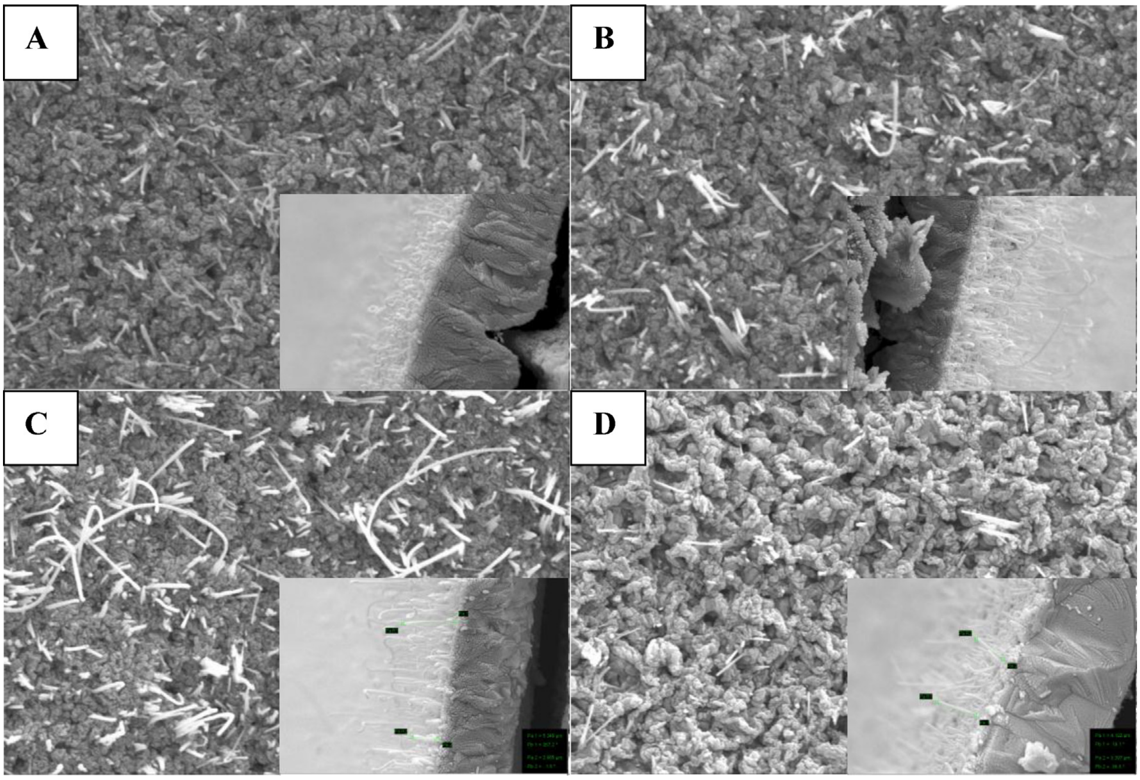

Fig. 6. SEM images of the support monoliths obtained by thermal treatment: (A) WO55; (B) WO515; (C) WO530 and (D) WO615. Atmosphere: wet oxygen. Temperature: 500 and 600 °C and time: 5, 15 and 30 min.

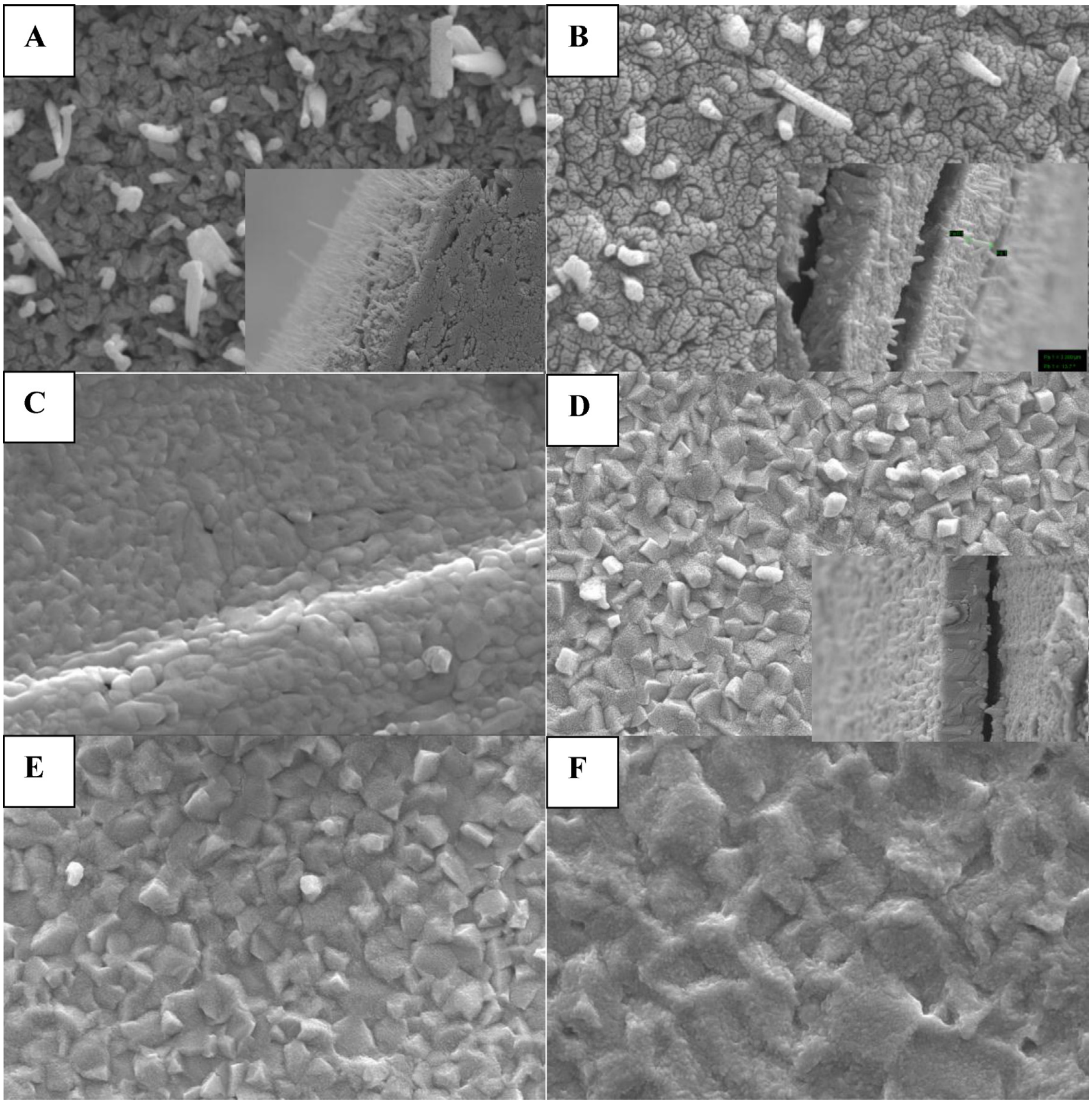

Fig. 7. SEM images of the support monoliths obtained by thermal treatment: (A) S55; (B) S515; (C) S530; (D) S65; (E) S615 and (F) S630. Atmosphere: stagnant. Temperature: 500 and 600 °C and time: 5, 15 and 30 min.

For support 530, X-ray diffraction showed only lines corresponding to the Cu_2O (PDF 5-667) phase. For the rest of the supports, besides Cu_2O (PDF 5-667), the most present phase, CuO (PDF 5-661) was also identified. Fig. 8 shows the diffractograms of the most representative supports for each condition of treatment.

Xu et al. [33] identified the phase Cu_2O in the samples treated in N_2 atmosphere, dry and wet. For the rest of the atmospheres, air and oxygen, they identified the two copper oxides – Cu_2O and CuO. The greater intensity of diffraction lines of Cu_2O phase in comparison with CuO may be explained by the partial pressure of oxygen present in each atmosphere. High partial pressures of oxygen favour the formation of nanostructures which exist under the form of CuO phase. The Cu–O phase diagram [42] shows that two types of oxides may be formed during the oxidation – Cu_2O and CuO. Thermodynamically, oxides are formed if the oxygen partial pressure of the environment (P_{O_2}) is higher than the pressure of dissociation ($P_{O_2\text{-dis.}}$) of the oxide in equilibrium with Cu, as shown in Eqs. (4) and (5):

$$2\,Cu + \frac{1}{2}\,O_2 = Cu_2O \tag{4}$$

$$Cu + \frac{1}{2}\,O_2 = CuO \tag{5}$$

The pressures of dissociation ($P_{O_2\text{-dis.}}$) for Cu_2O and CuO are 3×10^{-17} atm and 1×10^{-13} atm, respectively [33]. As can be observed, the dissociation pressure of CuO is higher than that of Cu_2O. Consequently, the formation of Cu_2O phase as the majority product of oxidation in stagnant atmosphere is due to the fact that the small amounts of oxygen present have P_{O_2} close to $P_{O_2\text{-dis.}}$ of Cu_2O, below the pressure of formation of CuO. This is in line with the observations of Xu et al. [33] for a N_2 atmosphere with traces of O_2. However, when the copper foils were oxidized in air or oxygen with $P_{O_2} = 0.22$ and 1, respectively, both copper oxides were formed in different ratios.

In all the supports, the treatment conditions applied caused modifications of the foil surface which provide the roughness and porosity necessary for its subsequent use as support of the active phase. However, working with corrugated foils, a detachment of the oxide layer was observed, with the exception of the foil treated in stagnant atmosphere at 500 °C for 30 min (530). Clearly, there is a deformation by tension in the corrugated foils where the corrosive

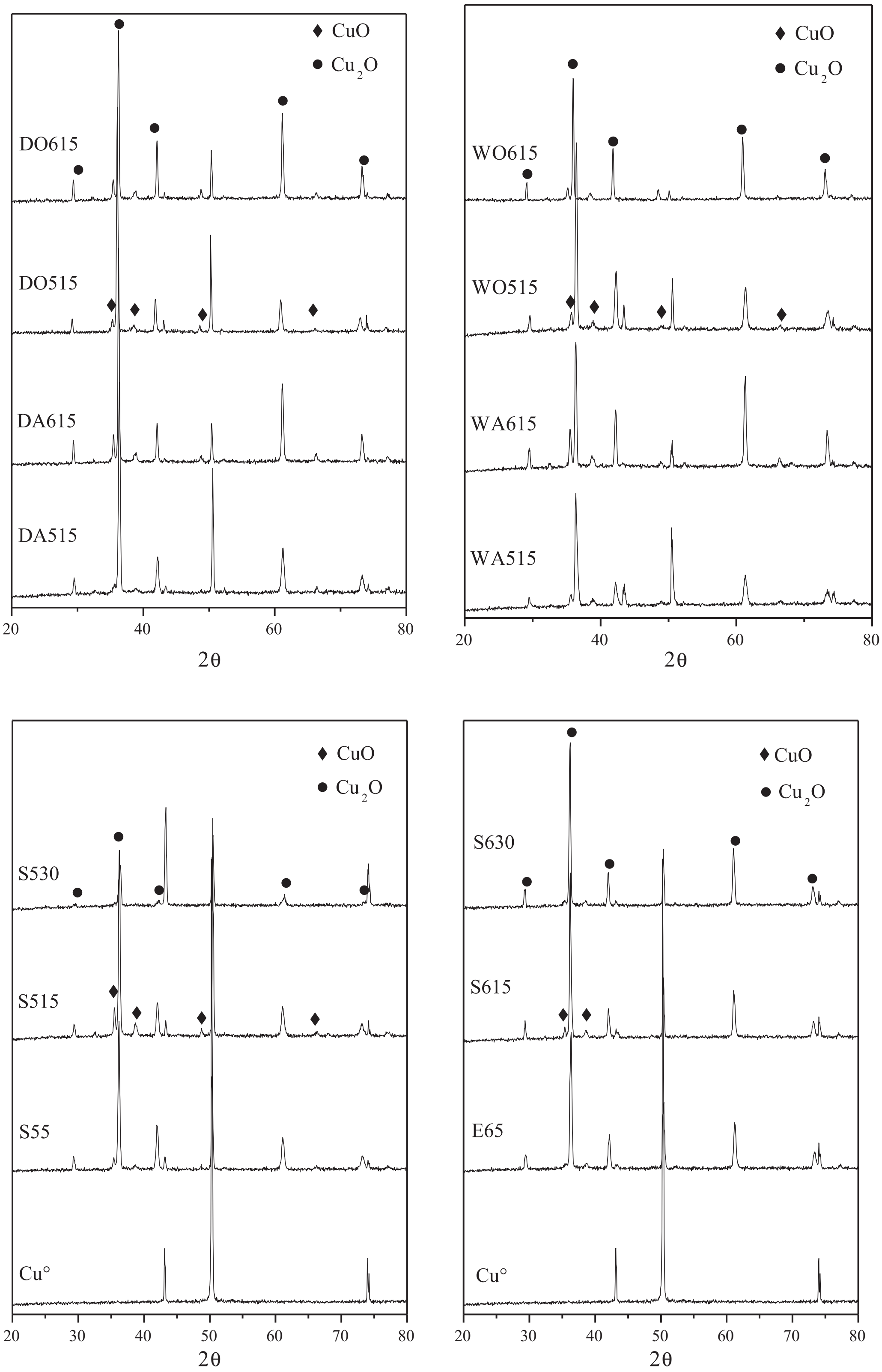

Fig. 8. XRD patterns of the support monoliths obtained by thermal treatment.

attack is more vigorous, weakening the adhesion of the oxide layer to the substrate. Based on this information, only monolith 530 was selected as support monolith.

The nano/microstructures generated by both treatments showed to be resistant to strong vibration shocks to which they were subjected during the adherence test. As can be seen in Table 3, weight losses are less than 6% wt. The SEM micrograph for one of the supports after the adherence test corroborates this low weight loss. Fig. 9 shows that most of nano/microstructures are preserved after the adherence test, being worn out only.

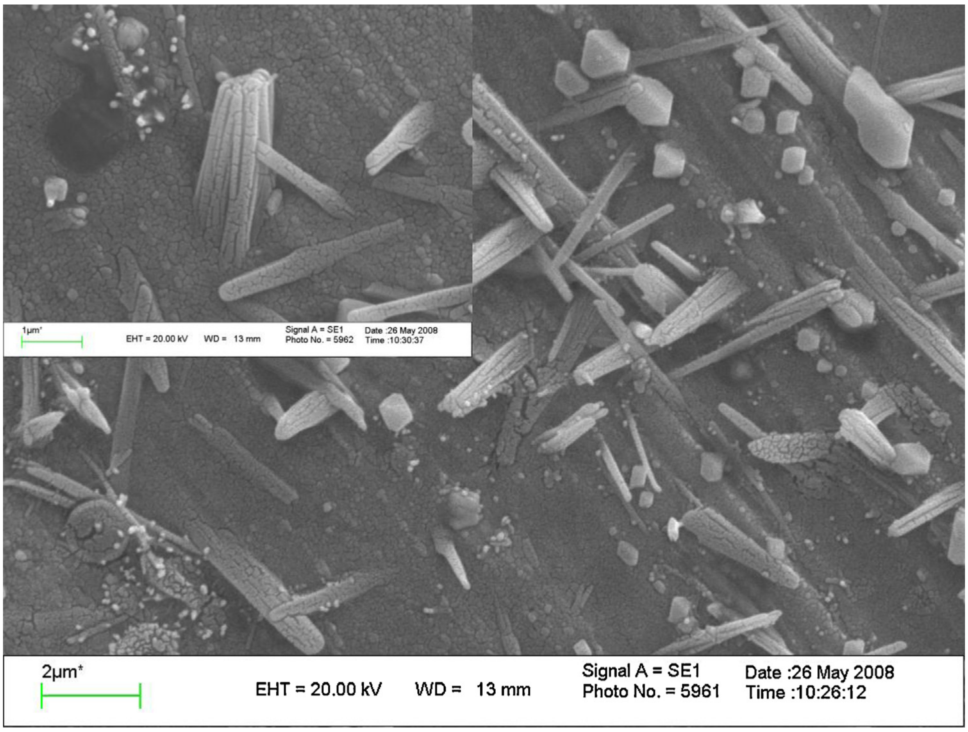

Fig. 9. SEM image of 10-6-24 support monolith after adherence test.

As expected, the surface areas for these supports are very low since the generated roughness is at micrometric scale (Table 3), but they are higher than the geometric area calculated for the untreated monolith of 0.00424 $m^2 g^{-1}$.

In general terms, we may say that the surface textures obtained in the 6 supports by both treatments are stable and suitable for the physical anchorage of catalyst particles. In addition, the nano/microstructures obtained can act directly as catalytic phase. Consequently, we decided to deposit a Mn–Cu mixed catalyst already optimized, (Mn9Cu1) [24], by washcoating on two of the supports (10-2-24 and 530). The monolithic catalysts were then evaluated in the complete combustion of toluene. These monoliths were named as 10-2-24 + Mn9Cu1 and 530 + Mn9Cu1. The supports monoliths 10-2-24 and 530 were also evaluated in the same reaction. Previous to the catalytic evaluation, the support 10-2-24 was calcined at 500 °C to obtain a stable phase during the evaluation. As can be seen in Fig. 10, the copper nano/microstructures preserve their form after calcinations, being composed by the same phase (Cu_2O).

Table 3 shows that a great amount of active phase was deposited by washcoating on both supports, presenting the same good adherence with a loss percentage lower than 3%. These results verify that the surface structure generated by both treatments is appropriate for acting as anchorage of Mn9Cu1 catalyst particles.

Table 3
Adherence test. Amount of the phase and surface area (S_{BET}).

Monolith	Adherence test (%)	S_{BET} (m^2 $monolith^{-1}$)	Amount of deposited phase (g)
10-1-24	6.2	1.48	
10-2-24	5.8	0.19	
10-2-40	6.1	0.09	
10-6-24	6.1	0.11	
40-2-40	6.2	0.17	
S530	5.9	0.32	
10-2-24 + Mn9Cu1	1.12	3.55	0.45
S530 + Mn9Cu1	2.52	6.51	0.48

The catalytic behaviour shown by those monoliths containing Mn9Cu1 catalyst is the expected for this catalyst, and it is comparable to the behaviour observed for this catalyst deposited on FeCrAlloy monoliths [43] (Fig. 11). Both supports show a similar behaviour, and the slight increase of activity shown by 530 + Mn9Cu1 monolith may be attributed to a higher content of the active phase.

When the copper nanostructures generated acted as active phase (Fig. 11), those obtained by thermal treatment were more active than those obtained by chemical treatment, but they were always less active than the optimized Mn9Cu1 catalyst. Nonetheless, the activity of these supports was considerable, taking into account that it was a single phase present in a low amount. It is considered that these monoliths exhibited good catalytic performance since the amount of active phase, generated in situ, is

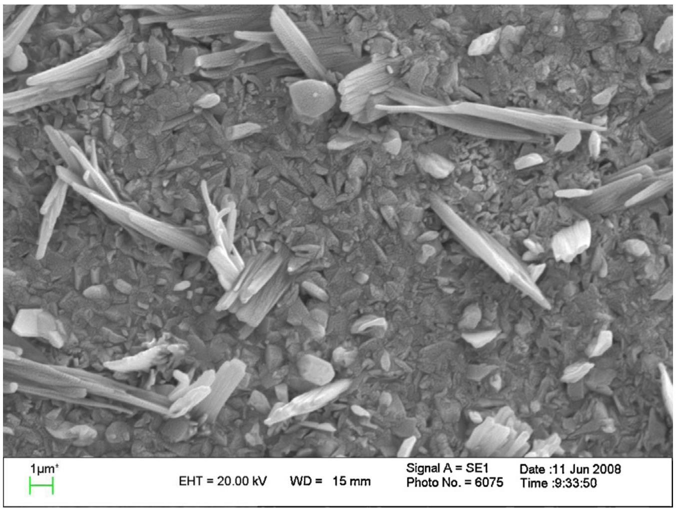

Fig. 10. SEM image of 10-2-24 support monolith calcined at 500 °C.

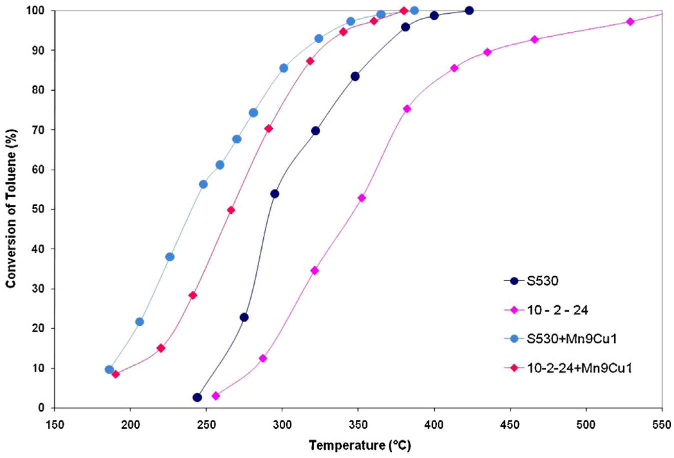

Fig. 11. Conversion of toluene as a function of the reaction temperature on 10-2-24 + Mn9Cu1, S530 + Mn9Cu1, 10-2-24 and S530 monoliths.

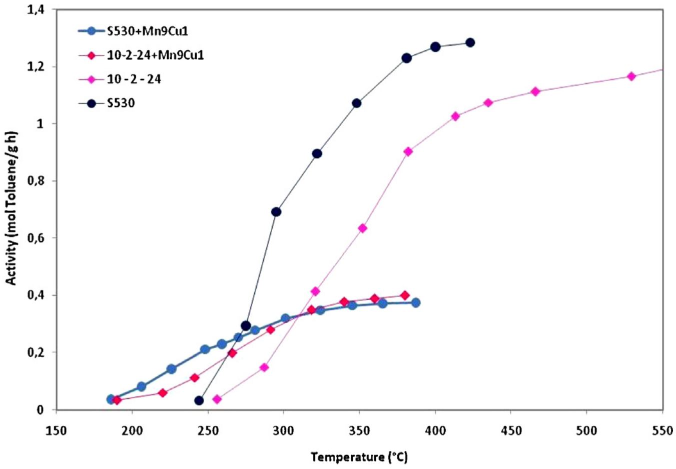

Fig. 12. Intrinsic catalytic activity of toluene as a function of the reaction temperature on 10- 2-24 + Mn9Cu1, S530 + Mn9Cu1, 10-2-24 and S530 monoliths.

approximately 0.145 g that is about 3 times less than the amount of Mn9Cu1 catalyst deposited by washcoating. The above mentioned can be appreciated in Fig. 12, intrinsic catalytic activity vs. temperature, which becomes independent of the amount of active phase. These results demonstrate the potentiality of the generated phases by both treatments to act as active phases, and also the possibility of being optimized to increase their catalytic activity.

4. Conclusions

By the systematic study of a wide range of variables of surface corrosion of Cu foils, the best conditions for their use as catalytic support were found.

The variables selected for the chemical and thermal treatments, applied to metallic copper monoliths generated stable copper nano/microstructures, appropriate for the catalytic objectives proposed in this work. The surface architecture achieved allowed to deposit by washcoating an acceptable and stable amount of Mn9Cu1 catalyst. The catalytic activity of these monoliths was equal to that exhibited by the Mn9Cu1 catalyst deposited on another metallic support. The copper phases generated by both treatments showed an acceptable catalytic behaviour in toluene combustion. The results obtained demonstrate the potentiality that these phases have to act as catalytic phase, and especially the possibility to be optimized in order to increase their performance.

Acknowledgement

The financial support from CONICET, Universidad Nacional de San Luis, ANPCyT is gratefully acknowledged.

References

[1] M. Baldi, F. Finocchio, F. Milella, G. Busca, Applied Catalysis B 16 (1998) 43–51.
[2] C. Lahousse, A. Bernier, P. Grange, B. Delmos, P. Papaefthimiou, T. Loannides, X. Verykios, Journal of Catalysis 178 (1998) 214–220.
[3] D.A. Hickman, L.D. Schmidt, Journal of Catalysis 138 (1992) 267–270.
[4] A. Paúl, Ph.D. Thesis, Instituto de Ciencias de los Materiales, Universidad de Sevilla, 1997.
[5] P. Avila, M. Montes, E. Miró, Chemical Engineering Journal 109 (2005) 11–36.
[6] L.C. Almeida, O. Gonzalez, O. Sanz, A. Paul, M.A. Centeno, J.A. Odriozola, M. Montes, Studies in Surface Science and Catalysis 167 (2007) 79–84.
[7] L.M. Martinez, D.M. Frias, M.A. Centeno, A. Paul, M. Montes, J.A. Odriozola, Chemical Engineering Journal 136 (2008) 390–397.
[8] O. Sanz, L.M. Martinez, F.J. Echave, M.I. Domínguez, M.A. Centeno, J.A. Odriozola, M. Montes, Chemical Engineering Journal 151 (2009) 324–332.
[9] O. Sanz, L.C. Almeida, J.M. Zamaro, M.A. Ulla, E.E. Miró, M. Montes, Applied Catalysis B 78 (2008) 166–175.
[10] Y. Li, Z. Zhang, X. Hong, Y. Liu, Catalysis Communications 9 (2008) 1040–1044.
[11] J.A. Hodges, Y. Sidis, P. Bourges, I. Mirebeau, M. Hennion, X. Chaud, Physical Review B 66 (2002) 020501 (R).
[12] X.G. Zheng, C.N. Xu, Y. Tomokiyo, E. Tanaka, H. Yamada, Y. Soejima, Physical Review Letters 85 (2000) 5170–5173.
[13] J. Tamaki, K. Shimanoe, Y. Yamada, Y. Yamamoto, N. Miura, N. Yamazoe, Sensors and Actuators, B 49 (1998) 121–125.
[14] T. Ishihara, M. Higuchi, T. Takagi, M. Ito, H. Nishiguchi, Y. Takita, Journal of Materials Chemistry 8 (9) (1998) 2037–2042.
[15] J.B. Reitz, E.I. Solomon, Journal of the American Chemical Society 120 (1998) 11467–11478.
[16] J. Ziolo, F. Borsa, M. Corti, A. Rigamonti, F. Parmigiani, Journal of Applied Physics 67 (1990) 5864–5867.
[17] X.P. Gao, J.L. Bao, G.L. Pan, H.Y. Zhu, P.X. Huang, F. Wu, D.Y. Song, Journal of Physical Chemistry B 108 (2004) 5547–5551.
[18] X.C. Jiang, T. Herricks, Y.N. Xia, Nano Letters 2 (2002) 1333–1338.
[19] Q. Liu, Y.Y. Liang, H.J. Liu, J.M. Hong, Z. Xu, Materials Chemistry and Physics 98 (2006) 519–522.
[20] Y. Chang, H.C. Zeng, Crystal Growth and Design 4 (2004) 397–402.
[21] R.A. Zarate, F. Hevia, S. Fuentes, V.M. Fuenzalida, A. Zuniga, Journal of Solid State Chemistry 180 (2007) 1464–1469.
[22] W.X. Zhang, S.X. Ding, Z.H. Yang, A.P. Liu, Y.Q. Qian, S.P. Tang, S.H. Yang, Journal of Crystal Growth 291 (2006) 479–484.
[23] M. Morales, B. Barbero, L. Cadús, Applied Catalysis B 67 (2006) 229–236.
[24] M. Morales, B. Barbero, L. Cadús, Fuel 87 (2008) 1177–1786.
[25] M. Kaur, K.P. Muthe, S.K. Despande, S. Choudhury, J.B. Sing, N. Verma, S.K. Gupta, J.V. Yakhmi, Journal of Crystal Growth 289 (2006) 670–675.
[26] L. Yu, G. Zhang, Y. Wu, X. Bai, D. Guo, Journal of Crystal Growth 310 (2008) 3125–3130.
[27] Q.M. Pan, H.Z. Jin, H.B. Wang, Nanotechnology 18 (2007) 355605.
[28] B. Balamurugan, B. Mehta, S. Shivaprasad, Applied Physics Letters 79 (2001) 3176–3178.
[29] W. Zhang, X. Wen, S. Yang, Inorganic Chemistry 42 (2003) 5005–5014.
[30] D. Shang, K. Yua, Y. Zhang, J. Xu, J. Wua, Y. Xu, L. Li, Z. Zhu, Applied Surface Science 255 (2009) 4093–4096.
[31] C.H. Xu, C.H. Woo, S.Q. Shi, Chemical Physics Letters 399 (2004) 62–66.
[32] B.J. Hansen, G. Lu, J. Chen, Journal of Nanomaterials (2008) 7, http://dx.doi.org/10.1155/2008/830474, Article ID 830474.
[33] C.H. Xu, C.H. Woo, S.Q. Shi, Superlattices and Microstructures 36 (2004) 31–38.
[34] R. Haugsrud, Journal of the Electrochemical Society 149 (2002) 14–21.
[35] J.T. Chen, F. Zhang, J. Wang, G.A. Zhang, B.B. Miao, X.Y. Fan, D. Yan, P.X. Yan, Journal of Alloys and Compounds 454 (2008) 268–273.
[36] L.S. Huang, S.G. Yang, T. Li, B.X. Gu, Y.W. Du, Y.N. Lu, S.Z. Shi, Journal of Crystal Growth 260 (2004) 130–135.
[37] B. Barbero, L. Costa-Almeida, O. Sanz, M. Morales, L. Cadus, M. Montes, Chemical Engineering Journal 139 (2008) 430–435.
[38] M. Valentini, G. Groppi, C. Crisitani, M. Levi, E. Tronconi, P. Forzatti, Catalysis Today 69 (2001) 307–314.
[39] S. Lv, H. Suo, C. Wang, S. Jing, T. Zhou, Y. Xu, J. Wang, C. Zhao, Solid State Communications 149 (2009) 404–407.
[40] S. Jana, S. Das, N.S. Das, K.K. Chattopadhyay, Materials Research Bulletin 45 (2010) 693–698.
[41] R.C. Wang, C.H. Li, Crystal Growth and Design 9 (2009) 2229–2234.
[42] T.B. Massalski, Binary Alloy Phase Diagrams, vol. 2, 2nd edition, ASM International, USA, 1999, pp. 1447.
[43] M. Morales, B. Barbero, L. Cadus, Catalysis Letters 141 (2011) 1598–1607.